



ARTICLE

Shikonin attenuates hyperhomocysteinemia-induced CD4⁺ T cell inflammatory activation and atherosclerosis in ApoE^{-/-} mice by metabolic suppression

Si-lin Lü^{1,2}, Guo-hui Dang¹, Jia-cheng Deng¹, Hui-ying Liu¹, Bo Liu¹, Juan Yang¹, Xiao-long Ma¹, Yu-tong Miao¹, Chang-tao Jiang¹, Qing-bo Xu³, Xian Wang¹ and Juan Feng^{1,4}

T cell metabolic activation plays a crucial role in inflammation of atherosclerosis. Shikonin (SKN), a natural naphthoquinone with anti-inflammatory activity, has shown to exert cardioprotective effects, but the effect of SKN on atherosclerosis is unclear. In addition, SKN was found to inhibit glycolysis via targeting pyruvate kinase muscle isozyme 2 (PKM2). In the present study, we investigated the effects of SKN on hyperhomocysteinemia (HHcy)-accelerated atherosclerosis and T cell inflammatory activation in ApoE^{-/-} mice and the metabolic mechanisms in this process. Drinking water supplemented with Hcy (1.8 g/L) was administered to ApoE^{-/-} mice for 2 weeks and the mice were injected with SKN (1.2 mg/kg, i.p.) or vehicle every 3 days. We showed that SKN treatment markedly attenuated HHcy-accelerated atherosclerosis in ApoE^{-/-} mice and significantly decreased inflammatory activated CD4⁺ T cells and proinflammatory macrophages in plaques. In splenic CD4⁺ T cells isolated from HHcy-ApoE^{-/-} mice, SKN treatment significantly inhibited HHcy-stimulated PKM2 activity, interferon- γ secretion and the capacity of these T cells to promote macrophage proinflammatory polarization. SKN treatment significantly inhibited HHcy-stimulated CD4⁺ T cell glycolysis and oxidative phosphorylation. Metabolic profiling analysis of CD4⁺ T cells revealed that Hcy administration significantly increased various glucose metabolites as well as lipids and acetyl-CoA carboxylase 1, which were reversed by SKN treatment. In conclusion, our results suggest that SKN is effective to ameliorate atherosclerosis in HHcy-ApoE^{-/-} mice and this is at least partly associated with the inhibition of SKN on CD4⁺ T cell inflammatory activation via PKM2-dependent metabolic suppression.

Keywords: atherosclerosis; shikonin; naphthoquinone; hyperhomocysteinemia; CD4⁺ T cell; metabolic suppression; ApoE^{-/-} mice

Acta Pharmacologica Sinica (2020) 41:47–55; <https://doi.org/10.1038/s41401-019-0308-7>

INTRODUCTION

Atherosclerosis, a chronic inflammatory cardiovascular disease, is the most common underlying cause of ischemic heart disease and stroke and carries a high mortality rate [1]. Homocysteine (Hcy) is a sulfur-containing amino acid formed during the metabolism of methionine. Elevated levels of plasma Hcy result in a condition known as hyperhomocysteinemia (HHcy), which has long been suggested as an independent risk factor for atherosclerosis [2, 3]. T cells can release cytokines and cooperate with other immune cells, such as B cells and macrophages, to mediate HHcy-accelerated inflammation and atherosclerosis [4, 5]. The metabolic activation of immune cells plays a key role in the inflammation of atherosclerosis. However, there are almost no natural and effective molecular therapies targeting T cell immunometabolism for HHcy-accelerated atherosclerosis.

Shikonin (SKN), a naphthoquinone and the major phytochemical component isolated from the root of *Lithospermum erythrorhizon*, has long been shown to exert an anti-inflammatory effect [6]. As a potent inhibitor of pyruvate kinase

muscle isozyme 2 (PKM2), SKN induces tumor cell death by inhibiting the Warburg effect [7]. Given that cell metabolism is closely related to immune cell activation, an accumulating number of studies suggest that SKN exerts an anti-inflammatory effect by modulating macrophage metabolism [8, 9]. However, the effects of SKN on T cell function and cellular metabolism and the subsequent consequence of these effects on crosstalk between T cells and macrophages remain unclear. In addition, metabolite profiling in cells can provide a picture of the cells' phenotype, assisting in elucidating the metabolic regulatory mechanism of an intervention. The potential of metabolomics of the Huh7 human hepatoma cell line treated with SKN has been investigated, increasing knowledge of the mechanisms involved in the antitumor activity of SKN [10]. Considering the important regulatory role of metabolic programming in different cell types and T cell-mediated inflammation in atherosclerosis, the detailed alterations in the metabolites in T cells responding to SKN treatment using high-throughput metabolomics must be revealed.

¹Department of Physiology and Pathophysiology, School of Basic Medical Sciences, Peking University Health Science Center, Key Laboratory of Molecular Cardiovascular Science, Ministry of Education, Beijing 100191, China; ²State Key Laboratory of Bioactive Substances and Function of Natural Medicine, Institute of Materia Medica, Peking Union Medical College, Chinese Academy of Medical Sciences, Beijing 100050, China; ³Cardiovascular Division, BHF Centre for Vascular Regeneration, King's College London, London SE5 9NU, UK and ⁴Department of Integration of Chinese and Western Medicine, School of Basic Medical Sciences, Peking University, Beijing 100191, China
Correspondence: Xian Wang (xwang@bjmu.edu.cn) or Juan Feng (juanfeng@bjmu.edu.cn)

Received: 17 June 2019 Accepted: 6 September 2019
Published online: 13 October 2019

A few studies have suggested the cardioprotective effects of SKN related to its anti-inflammatory capacity, but most of these investigations focused on cardiac function or blood vessel contraction [6]. SKN was reported to inhibit tumor necrosis factor- α (TNF- α)-induced proliferation and invasion of rat vascular smooth muscle cells (VSMCs), indicating the potential anti-atherosclerotic effect of SKN [11]. The aim of the current study was to investigate the precise effects of SKN on HHcy-induced atherosclerosis and T cell inflammatory activation and reveal the metabolic mechanism involved in this process. These results identify SKN as a potential natural agent against atherosclerosis.

MATERIALS AND METHODS

Materials

Hcy, SKN, oligomycin, carbonyl cyanide 4-(trifluoromethoxy) phenylhydrazone (FCCP), rotenone (Rot), and antimycin A (Anti A) were obtained from Sigma Chemical Co. (St. Louis, MO, USA). RPMI-1640 medium was obtained from Gibco (Gaithersburg, MD, USA). Fetal bovine serum (FBS) was obtained from Gemini Bio-Products (West Sacramento, CA, USA). Brefeldin A was purchased from BioLegend (San Diego, CA, USA). Antibodies against eukaryotic translation initiation factor-5 (eIF5) and inducible nitric oxide synthase (iNOS) were obtained from Santa Cruz Biotechnology (CA, USA). An antibody against acetyl-CoA carboxylase 1 (ACC1) was obtained from Cell Signal Technology (Danvers, MA, USA). An antibody against F4/80 was purchased from Abcam (Cambridge, MA, USA). Antibodies against CD4, CD28, and interferon (IFN)- γ were purchased from BD Pharmingen (Franklin Lakes, NJ, USA). An antibody against β -actin was purchased from Easy Bio (Beijing, China).

Animals and treatment

Six-week-old pathogen-free female C57BL/6J mice and ApoE^{-/-} mice were provided by the Animal Center of Peking University Health Science Center (Beijing, China). The animals were randomized for treatment.

ApoE^{-/-} mice acclimatized to the laboratory for 7 days were randomly assigned to one of the four groups. These groups were a vehicle control group (CTL, solvent injection every 3 days), HHcy-induced atherosclerosis group (HHcy, solvent injection plus Hcy in drinking water for 2 weeks), only SKN-treated group (1.2 mg/kg SKN injection every 3 days), and SKN- and Hcy-treated group (SKN injection plus Hcy in drinking water). SKN was dissolved in dimethyl sulfoxide (DMSO) at a concentration of 6 mg/mL and then diluted in phosphate-buffered saline (PBS) to a final concentration of 0.12 mg/mL for further injection. DMSO at dilutions similar to those of SKN was used as the solvent. Mice received a final injection volume of 1% of their body weight. ApoE^{-/-} mice were first intraperitoneally injected with 1.2 mg/kg SKN (Sigma Chemical Co., USA) or solvent one time. Three days after the first injection, the mice were administered 1.8 g/L Hcy (Sigma Chemical Co., USA) in their drinking water for 2 weeks. During this process, mice were continuously injected with SKN or solvent every 3 days. Serial sections of dissected aortic roots were used for oil red O staining, immunofluorescence staining, and immunohistochemical staining. Splenic CD4⁺ T cells were isolated from individual mice and ex vivo activated with anti-CD3 (1 μ g/mL, BD Pharmingen, USA) for 24 h for further analysis.

All mice were anesthetized with isoflurane (2%) and euthanized by cervical dislocation. The protocol was approved by the Committee on the Ethics of Animal Experiments of the Health Science Center of Peking University. The investigation conformed to the Guide for the Care and Use of Laboratory Animals published by the US National Institutes of Health (NIH Publication, 8th Edition, 2011).

CD4⁺ T cell isolation and culture

CD4⁺ T cells from mouse spleens were purified by positive selection according to the manufacturer's protocol (STEMCELL Technologies, Inc., Vancouver, BC, Canada) as we previously reported [12]. Purified CD4⁺ T cells were suspended in RPMI-1640 medium (Gibco, USA) supplemented with 10% FBS and seeded in plates precoated with anti-CD3 antibody (1 μ g/mL, BD Pharmingen, USA). Cells were incubated at 37 °C in a 5% CO₂ incubator for the indicated times. SKN (0.05–0.25 μ M) was added 30 min prior to the 24 h Hcy treatment.

Coculture experiments

The macrophages were isolated as described in our previous published paper [13]. The main isolation steps were as follows: 6-week-old C57BL/6J female mice were injected intraperitoneally with 2 mL of 4% thioglycollate broth (BD Biosciences Clontech, CA, USA). Three days later, the mice were anesthetized with isoflurane (2%) and euthanized by cervical dislocation. Macrophages were obtained by peritoneal lavage with 8 mL of cold PBS supplemented with 10 mM EDTA and 10% FBS. Cells were plated in RPMI 1640 medium with 10% FBS. After incubation for 2 h at 37 °C, nonadherent cells were washed away, and adherent cells were cultured for another 12 h before further experiments. CD4⁺ T cells were pretreated with SKN (0.2 μ M) for 30 min followed by stimulation with or without Hcy (100 μ M) for 24 h in the presence of anti-CD3 antibody and then collected and resuspended in fresh RPMI-1640 medium with 10% FBS. Finally, the macrophages were cocultured with CD4⁺ T cells in fresh RPMI-1640 medium for the indicated times (12 h for mRNA analysis and 24 h for protein analysis). As macrophages are adherent cells and CD4⁺ T cells are suspended cells, we could specifically detect proteins or mRNAs from macrophages by washing away CD4⁺ T cells with PBS.

Mitochondrial respiration and cell glycolysis assays

Oxygen consumption rate (OCR, in pmol/min) and extracellular acidification rate (ECAR, in mpH/min) of splenic CD4⁺ T cells were analyzed using a Seahorse XF-24 metabolic extracellular flux analyzer (Seahorse Bioscience, Billerica, MA, USA) as we previously reported [12]. CD4⁺ T cells were first treated with the indicated reagents for 24 h and then harvested and resuspended in XF Base Medium (Seahorse Bioscience, USA) supplemented with 11 mM glucose, 1 mM pyruvate, and 2 mM glutamine. CD4⁺ T cells were then seeded at a density of 10⁶ cells/well in 24-well XF microplates coated with poly-L-lysine hydrobromide (Sigma Chemical Co., USA). After incubation in a CO₂-free incubator at 37 °C for 1 h, basal metabolism and metabolism in response to mitochondrial inhibitors [1 μ M oligomycin, 1 μ M FCCP, and 1 μ M Rot+1 μ M Anti A (Sigma Chemical Co., USA)] were analyzed. The assay conditions were as follows: 3 min of mixing; a 2 min wait; and 3 min of measurement. Metabolic parameters were then calculated. OCR and ECAR were normalized to the cell number in each well.

Analysis of metabolites

Water-soluble metabolites in CD4⁺ T cells (3 \times 10⁷ per sample) were analyzed using liquid chromatography tandem mass spectrometry (LC-MS/MS) as we previously reported [12]. After the indicated treatments, CD4⁺ T cells were harvested, washed with ice-cold saline, and then lysed in 1 mL of 80% methanol by freezing and thawing. The supernatants were collected and evaporated. The residues were dissolved in 120 μ L of tri-distilled water prior to LC-MS/MS analysis.

Lipid analysis was performed as we previously reported [12]. After the indicated treatments, CD4⁺ T cells (10⁷ per sample) were washed and homogenized in 100 μ L of saline and then extracted with a solution of methanol and chloroform at a ratio of 1:2. The organic layer was isolated and dried. The residues were resuspended in a solution of isopropanol:acetonitrile (1:1) prior to LC-MS/MS analysis.

Metabolite abundance was normalized using internal standards and the cell number. MetaboAnalyst was used for heat map analysis.

PKM2 activity analysis

CD4⁺ T cells (5×10^6 per sample) treated as indicated were washed and lysed in pyruvate kinase (PK) lysis buffer on ice for 30 min. The supernatant was collected and used for PKM2 activity analysis using a continuous assay coupled to lactate dehydrogenase (LDH) as previously reported [14]. Two micrograms of cell lysate (0.2 µg/µL) was mixed with 190 µL of PK assay buffer (50 mM Tris (pH 7.5), 100 mM KCl, 5 mM MgCl₂, 0.6 mM ADP, 0.5 mM phosphoenolpyruvate, 540 µM NADH, 200 µM fructose-1,6-bisphosphate, and 8 units LDH). PKM2 activity at 25 °C was calculated by monitoring changes in absorbance at 340 nm from 0 to 20 min using a Varioskan Flash Multimode Reader (Thermo Fisher Scientific, Waltham, MA, USA).

Quantitative reverse transcriptase PCR

Total RNA was isolated using TRIzol reagent (Invitrogen, Carlsbad, CA, USA) and reversed transcribed with a reverse transcription system (Promega, Madison, WI, USA). Then the reaction mixture was subjected to PCR. The primer sequences used for PCR analyses based on mouse genes were as follows: β-actin (forward, 5'-GTGACGTTGACATCCGTAAG-3'; reverse, 5'-GCCGGACTCATCGTACTCC-3'), iNOS (forward, 5'-TGCATGGACCAGTATAAGGCA-3'; reverse, 5'-GCTTCTGGTCGATGCATGAGCAA-3'), CD80 (forward, 5'-AAGTGGTGTCTGTCTGCATT-3'; reverse, 5'-TAATGGTGTGGTTGCAGATC-3'), and CD86 (forward, 5'-ATGGGCTCGTATGATTGT-3'; reverse, 5'-CTTCTTAGGTTTCGGGTG-3'). The amount of PCR product formed in each cycle was evaluated by SYBR Green I fluorescence. Amplification reactions were performed using an Mx3000 Multiplex Quantitative PCR System (Stratagene, La Jolla, CA). The data were analyzed with the Stratagene Mx3000 software.

Western blot analysis

Total protein was collected in cell lysis buffer (Beyotime, Jiangsu, China) containing 1 mM phenylmethylsulfonyl fluoride, 10 µg/mL aprotinin, 10 µg/mL pepstatin A, and 10 µg/mL leupeptin.

Proteins were quantified by bicinchoninic acid protein assay (Pierce Biotechnology, Rockford, USA) and then separated by 8% or 10% sodium dodecyl sulfate-polyacrylamide gel electrophoresis. Proteins on the blots were detected by special primary antibodies and the appropriate second antibodies. Images were obtained by an Odyssey infrared imaging system (LI-COR Biosciences, Lincoln, NE, USA).

Fluorescence-activated cell sorter

(a) Intracellular IFN-γ was detected as we previously reported [12]. Cells treated as indicated were first incubated with brefeldin A (5 µg/mL, BioLegend, USA) for 5 h before cell harvesting and then fixed and permeabilized using eBioscience Foxp3/Transcription Factor Staining Buffer Set (Thermo Fisher Scientific, USA) before finally being blocked and stained with APC-IFN-γ antibody (clone XMGI.2; BD Pharmingen, USA). (b) Cell death was detected by propidium iodide (PI) staining (Invitrogen, USA). Splenic CD4⁺ T cells treated with SKN and Hcy were resuspended at 10^7 /mL, and PI was added to a final concentration of 1 µg/mL in a volume of 100 µL per assay. After incubation at room temperature for 10 min, the cells were washed and assessed as soon as possible. (c) Data were acquired by a FACScalibur flow cytometer (BD Biosciences, USA) with the Cell QuestPro software (BD Bioscience, USA) and analyzed using the FlowJo software (Treestar, Ashland, OR, USA).

Morphometric analysis of atherosclerosis

Atherosclerotic lesion size was measured as we previously reported [15]. The aortic root was serially cross-sectioned at 7-

µm intervals, and every other section was collected on glass slides. Six sections spaced 70 µm apart and thus spanning 350 µm of the aortic root were stained with oil red O to visualize lesion areas. The plaque areas were calculated using ImageJ 1.37v (Wayne Rasband, National Institutes of Health, USA). The mean lesion size is presented. Immunofluorescence staining was used to detect CD28-expressing CD4⁺ T cells and proinflammatory macrophages (iNOS- and F4/80-positive). Immunohistochemical staining was used to detect macrophages (F4/80-positive) in atherosclerotic plaques.

Analysis of plasma Hcy, triglyceride, and cholesterol levels

The total plasma Hcy level was quantified by enzymatic cycling assay as previously described [16]. Plasma triglyceride and cholesterol levels were assayed using kits from Zhong Sheng Biotechnology (Beijing, China). Five microliters of plasma was mixed with the corresponding assay buffer at 37 °C for 10 min, and the absorbance was detected at 450 nm.

Statistical analysis

All experiments were randomized and blinded. All data are presented as mean ± SD. GraphPad Prism software was used for data analysis. The values were derived from a Gaussian distribution and tested by Shapiro–Wilk normality test. One-way analysis of variance followed by Tukey's test was used for multiple comparisons, and Student's unpaired *t* test was used for comparisons between two groups. *P* < 0.05 indicated statistical significance.

RESULTS

SKN attenuates the HHcy-induced CD4⁺ T cell and macrophage inflammatory response in atherosclerotic lesions in ApoE^{-/-} mice. We administered Hcy (1.8 g/L) in drinking water to ApoE^{-/-} mice for 2 weeks and intraperitoneally injected SKN (1.2 mg/kg) or solvent into the mice every 3 days (Fig. S1a). Consistent with the results of our previous study, SKN had no effect on the plasma Hcy level, body weight, and plasma cholesterol and triglyceride levels but significantly inhibited HHcy-accelerated atherosclerotic lesion formation (Fig. S1b–e) [4]. To further investigate the effect of SKN on HHcy-accelerated atherosclerosis in ApoE^{-/-} mice, we detected the inflammatory cell components of the atherosclerotic plaques. CD28 signaling is necessary to fully activate T lymphocytes [5, 17]. Here we found many more CD4⁺ T cells accompanied by increased CD28 expression in the atherosclerotic lesions of HHcy-ApoE^{-/-} mice than in control mice; this increase was completely reduced by SKN treatment, as indicated by immunofluorescence staining (Fig. 1a). Immunohistochemistry staining showed an increased number of macrophages in the atherosclerotic plaques of HHcy-ApoE^{-/-} mice, and this effect was also reduced significantly by SKN injection (Fig. 1b). Further detection showed that SKN reduced the expression of HHcy-promoted proinflammatory macrophage marker iNOS in the atherosclerotic plaques of ApoE^{-/-} mice (Fig. 1c). These results indicate that SKN ameliorates HHcy-accelerated atherosclerosis in ApoE^{-/-} mice and reduces the CD4⁺ T cell and macrophage inflammatory response in lesions.

SKN inhibits HHcy-induced CD4⁺ T cell IFN-γ secretion and subsequently reduces T cell-mediated proinflammatory macrophage polarization

We showed above that CD4⁺ T cells and proinflammatory macrophages were increased in the atherosclerotic plaques of HHcy-ApoE^{-/-} mice and that this effect was reduced by SKN treatment. In addition, we previously demonstrated that HHcy increased IFN-γ levels in the atherosclerotic plaques of ApoE^{-/-} mice [12]. Furthermore, IFN-γ was shown to mediate the polarization of macrophages to a proinflammatory state [18].

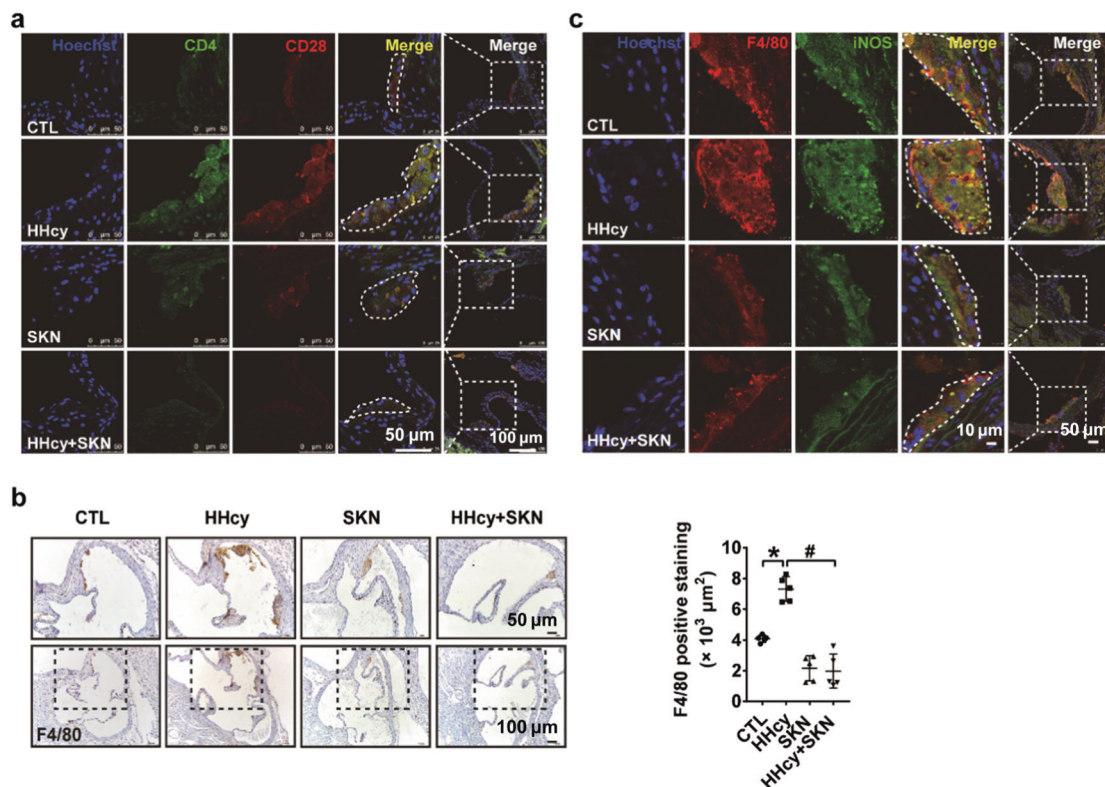


Fig. 1 SKN attenuates the HHcy-induced CD4⁺ T cell and macrophage inflammatory response in the atherosclerotic lesions of ApoE^{-/-} mice. HHcy was induced in ApoE^{-/-} mice by supplementing drinking water with Hcy (1.8 g/L) for 2 weeks. SKN (1.2 mg/kg) or solvent was intraperitoneally injected every 3 days. **a** Immunofluorescence staining for CD4 and CD28 in the plaques of aortic roots (*n* = 5 mice per group). **b** Macrophages (F4/80-positive) in the atherosclerotic plaques of aortic roots were detected by immunohistochemical staining. Quantification is shown in the right panel (*n* = 5 mice per group). **c** Immunofluorescence staining for F4/80 and iNOS in the plaques of aortic roots (*n* = 5 mice per group). The data are shown as mean ± SD. One-way ANOVA followed by Tukey's test was used for multiple comparisons. **P* < 0.05 compared with the CTL group; #*P* < 0.05 compared with the HHcy group

SKN may inhibit vascular inflammation by regulating the crosstalk between T cells and macrophages. To verify this hypothesis, we first investigated the exact effects of SKN on HHcy-stimulated CD4⁺ T cells in vivo. SKN injection indeed successfully reduced HHcy-induced elevated PKM2 activity (by approximately 37.0%) and IFN-γ secretion (by approximately 87.4%) in CD4⁺ T cells (Fig. 2a, b). Following these experiments, we designed relevant ex vivo coculture experiments to further explore the effects of T cells in different experimental groups on macrophage polarization. First, macrophages were isolated from normal C57BL/6J mice and maintained in resting medium. At the same time, splenic CD4⁺ T cells isolated from HHcy-ApoE^{-/-} mice with or without SKN treatment were ex vivo activated with anti-CD3 for 24 h. Then we cultured these ex vivo activated CD4⁺ T cells with the normal macrophages in fresh medium and subsequently detected the macrophage phenotype 12 h later. After coculture with CD4⁺ T cells isolated from HHcy-ApoE^{-/-} mice, proinflammatory gene (iNOS, CD80, and CD86) expression in macrophages was increased, and this phenomenon was abolished in macrophages cocultured with CD4⁺ T cells isolated from SKN-injected HHcy-ApoE^{-/-} mice (Fig. 2c).

Similar results were also observed in corresponding in vitro experiments. First, CD4⁺ T cells were pretreated with a dose titration of SKN (0.05–0.25 μM) for 30 min, and these cells were then stimulated with or without Hcy (100 μM) for an additional 24 h to confirm the efficient inhibitory concentration. Both 0.2 and 0.25 μM SKN significantly inhibited Hcy-induced increased PKM2 activity (Fig. 2d), while the cell death of CD4⁺ T cells was not affected by SKN (Fig. 2e). SKN (0.2 μM) efficiently inhibited Hcy-induced CD4⁺ T cell IFN-γ secretion, as detected by enzyme-linked

immunosorbent assay and FACS (Fig. 2f, g). Then we cocultured differently pretreated CD4⁺ T cells with normal macrophages in fresh medium for another 24 h. Coincubation with Hcy-simulated CD4⁺ T cells significantly increased the expression of the proinflammatory macrophage-associated protein iNOS by 53.3% in macrophages, which was reduced by 48.4% in macrophages cocultured with SKN-pretreated CD4⁺ T cells (Fig. 2h). Furthermore, Hcy-activated CD4⁺ T cell-induced proinflammatory macrophage polarization was reduced by IFN-γ neutralizing antibody, which confirmed that Hcy-activated CD4⁺ T cells mediate proinflammatory macrophage polarization by secreting IFN-γ (Fig. 2i). Therefore, these results indicate that SKN inhibits HHcy-induced CD4⁺ T cell inflammatory activation with decreased IFN-γ secretion, which leads to reduced proinflammatory macrophage polarization.

SKN inhibits HHcy-induced metabolic reprogramming in CD4⁺ T cells

PKM2-dependent metabolic reprogramming in CD4⁺ T cells is critical for HHcy-induced atherosclerosis in ApoE^{-/-} mice [12]. Does SKN inhibit the HHcy-induced CD4⁺ T cell inflammatory response by modulating cellular metabolism in vivo? The detailed metabolic phenotypes of HHcy-stimulated CD4⁺ T cells in the presence or absence of SKN injection were examined by an extracellular metabolic flux analyzer. ECAR is an indicator of aerobic glycolysis, and OCR is an indicator of oxidative phosphorylation (OXPHOS). SKN injection (1.2 mg/kg every 3 days) reduced the elevated basal ECAR (from 20.3 ± 4.6 to 13.3 ± 3.3 mpH/min) and OCR (from 207.9 ± 29.1 to 135.9 ± 43.8 pmol/min) following 2 weeks of Hcy treatment, which

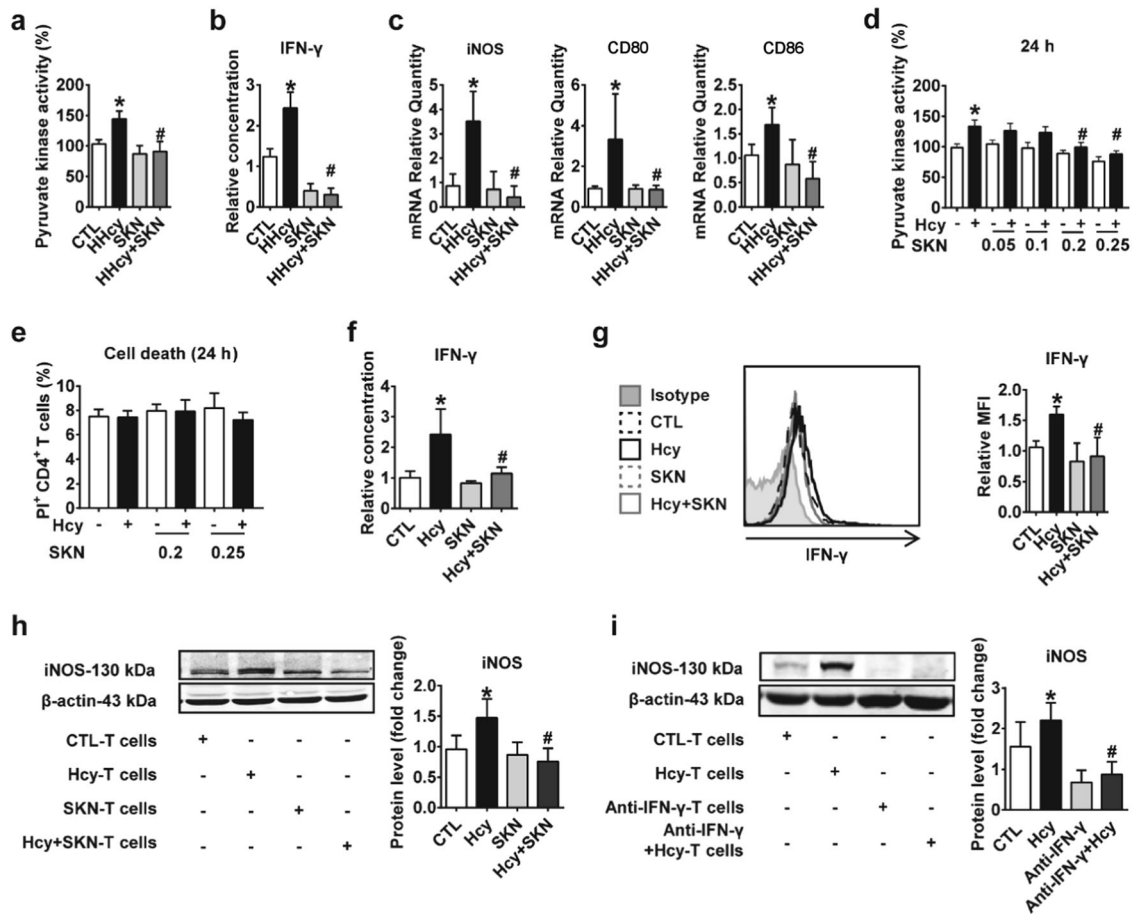


Fig. 2 SKN inhibits HHcy-induced IFN- γ secretion in CD4⁺ T cells and subsequently reduces T cell-mediated proinflammatory macrophage polarization. **a** Splenic CD4⁺ T cells isolated from CTL and HHcy mice treated with or without SKN (1.2 mg/kg) were stimulated with anti-CD3 (1 μ g/mL) for 24 h ex vivo. PKM2 activity was measured ($n = 6$ mice per group). **b** IFN- γ in the supernatant of splenic CD4⁺ T cells treated as in **a** was detected by ELISA ($n = 7$ mice per group). **c** Splenic CD4⁺ T cells treated as in **a** were cocultured with normal macrophages in fresh medium for 12 h. The mRNA levels of iNOS, CD80, and CD86 were detected by RT-PCR ($n = 7$ mice per group). **d–h** Splenic CD4⁺ T cells were first treated with SKN (0.05–0.25 μ M) for 30 min and then stimulated with or without Hcy (100 μ M) for 24 h. PKM2 activity is shown in **d** ($n = 5$). Cell death was detected by PI staining (**e**) ($n = 5$). IFN- γ secretion was detected by ELISA (**f**) ($n = 9$) and FACS (**g**) ($n = 5$). After treatment with SKN (0.2 μ M) and Hcy (100 μ M) for 24 h, these splenic CD4⁺ T cells were then cocultured with normal macrophages in fresh medium for another 24 h. The protein level of iNOS in macrophages was detected by Western blotting (**h**) ($n = 5$). **i** Splenic CD4⁺ T cells were stimulated with Hcy (100 μ M) for 24 h and then cocultured with normal macrophages in fresh medium in the presence of IFN- γ -neutralizing antibodies for another 24 h. The protein level of iNOS in macrophages was detected by Western blotting ($n = 5$). The data are shown as mean \pm SD. One-way ANOVA followed by Tukey's test was used for multiple comparisons. * $P < 0.05$ compared with the CTL group; # $P < 0.05$ compared with the HHcy or Hcy group

indicated that SKN inhibits glycolytic and oxidative metabolism (Fig. 3a, b). SKN also inhibited the HHcy-induced elevated maximal ECAR, reflecting an SKN-induced reduction in the maximal glycolytic potential (Fig. 3a). In vitro experiments showed similar results and indicated that SKN pretreatment inhibited the Hcy-induced increase in ECAR and OCR (Fig. 3c, d). These data indicate that the inhibition of HHcy-induced CD4⁺ T cell metabolic reprogramming may be the key mechanism by which SKN exerts protective effects against HHcy-induced inflammatory activation.

SKN inhibits Hcy-induced CD4⁺ T cell glucose metabolism

Detailed metabolic profiling can reveal key regulatory points in cells upon intervention. To further investigate the metabolic regulatory mechanism of SKN, we therefore examined various metabolite levels in Hcy-stimulated CD4⁺ T cells with or without SKN intervention in detail by the use of high-throughput LC-MS/MS. Consistent with the results of our previous study, Hcy stimulation led to the accumulation of upstream glycolytic

intermediates (Fig. 4a, d), downstream tricarboxylic acid (TCA) cycle intermediates (Fig. 4b, d), and intermediates of the pentose phosphate pathway (Fig. 4c, d). The accumulation in all these intermediates was successfully inhibited by SKN pretreatment (Fig. 4a–d). These findings indicate that SKN inhibits Hcy-induced CD4⁺ T cell glucose metabolism.

SKN inhibits Hcy-induced activation of the glycolytic–lipogenic axis in CD4⁺ T cells

Glucose metabolism provides carbon for de novo lipid synthesis via glycolysis and the TCA cycle [19]. Here we further analyzed the effect of SKN on Hcy-activated lipid synthesis. Lipidomics showed that Hcy significantly increased the load of various lipids, including phosphatidylcholine (PC) (Fig. 5a, d), phosphatidylethanolamine (PE) (Fig. 5b, d), and sphingomyelin (SM) (Fig. 5c, d) in CD4⁺ T cells. The Hcy-induced increase in all these accumulated lipids was reversed completely by SKN treatment (Fig. 5a–d). In addition, the Hcy-induced increase in ACC1, a crucial enzyme for de novo lipid synthesis, was reduced by SKN pretreatment (Fig. 5e). Therefore,

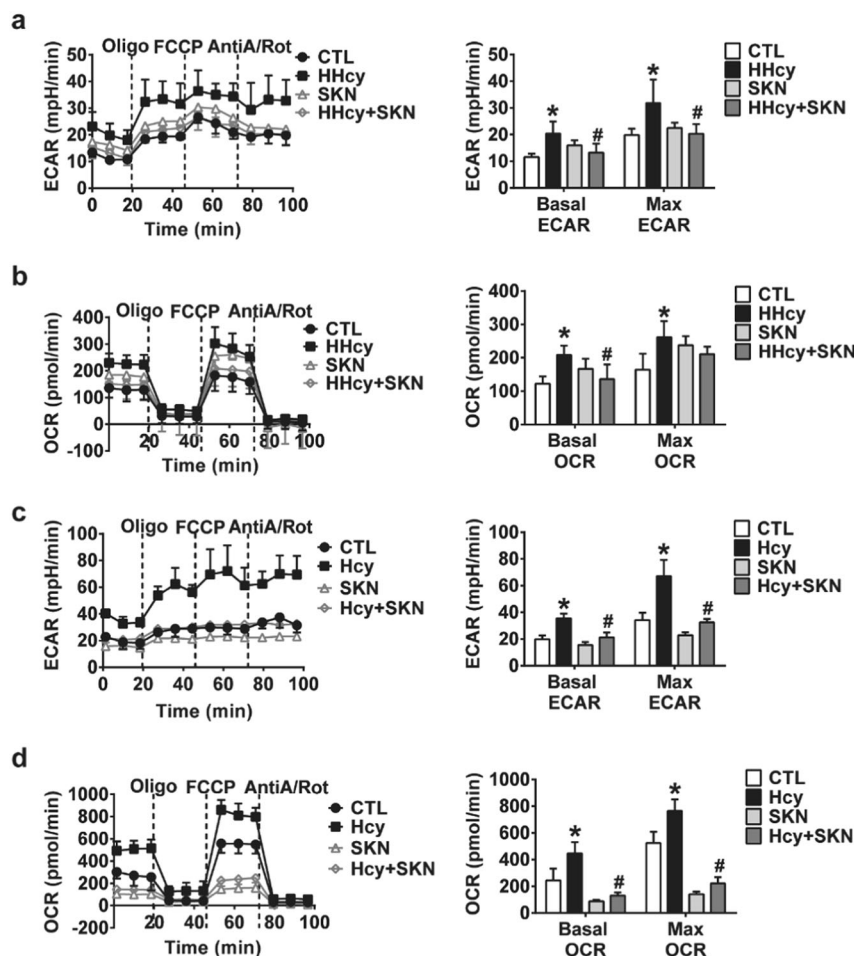


Fig. 3 SKN inhibits HHcy-induced metabolic reprogramming in CD4⁺ T cells. **a, b** Splenic CD4⁺ T cells isolated from CTL and HHcy mice treated with or without SKN (1.2 mg/kg) were stimulated with anti-CD3 (1 μg/mL) for 24 h ex vivo. ECAR and OCR were detected by extracellular flux analysis (*n* = 5 mice per group). Rot rotenone, Anti A antimycin A. **c, d** Splenic CD4⁺ T cells were treated with or without SKN (0.2 μM) for 30 min and then stimulated with or without Hcy (100 μM) for 24 h. ECAR and OCR were detected by extracellular flux analysis (*n* = 5). The data are shown as mean ± SD. One-way ANOVA followed by Tukey's test was used for multiple comparisons. **P* < 0.05 compared with the CTL group; #*P* < 0.05 compared with the HHcy or Hcy group

SKN inhibits Hcy-induced glycolytic–lipogenic axis activation in CD4⁺ T cells.

Figure 6 shows a working model of the mechanism by which SKN ameliorates atherosclerosis by inhibiting CD4⁺ T cell metabolic activation. Hcy enhances glucose metabolism and the glycolytic–lipogenic axis in CD4⁺ T cells to promote IFN-γ secretion, which promotes macrophage proinflammatory polarization and finally accelerates atherosclerosis. Inhibition of PKM2 by SKN prevents these effects.

DISCUSSION

In the present study, we investigated the effects of SKN on atherosclerosis and associated T cell inflammatory activation and verified the potential metabolic regulatory mechanisms of SKN. For the first time, SKN was shown to ameliorate atherosclerosis in HHcy-ApoE^{-/-} mice and inhibited CD4⁺ T cell-associated inflammatory responses in atherosclerotic plaques. Mechanistically, SKN inhibited HHcy-induced CD4⁺ T cell IFN-γ secretion and the capacity HHcy to promote macrophage proinflammatory polarization by decreasing the HHcy-induced increase in glycolysis and OXPHOS. More importantly, metabolomics revealed that SKN inhibited intermediate glucose metabolites and also reduced the accumulation of lipids in Hcy-activated CD4⁺ T cells. These results

indicate that SKN may be a promising natural therapeutic agent for the treatment of atherosclerosis, which might result from the anti-inflammatory effects of SKN by inhibiting CD4⁺ T cell metabolic activation (Fig. 6).

The precise regulatory effects of SKN in atherosclerosis have not been thoroughly investigated, although a few studies have suggested the cardioprotective effects of SKN. For example, SKN ameliorated isoproterenol-induced cardiac injury by decreasing myocardial fibrosis, suppressing inflammation, and attenuating apoptosis and endoplasmic reticulum stress [20]. SKN was also shown to exert antithrombotic and antifibrinolytic effects by inhibiting the activity of plasminogen activator inhibitor-1, which is a key negative regulator of the fibrinolytic system [21]. Regarding vascular function, SKN inhibited rat thoracic aortic relaxation in response to acetylcholine in a dose-dependent manner [22]. Using an accelerated HHcy-induced atherosclerotic animal model, the present study is the first to show the protective effect of SKN on atherosclerosis via a reduction in CD4⁺ T cell inflammatory activation; these results pave the way to explore the therapeutic potential of SKN in inflammatory vascular diseases.

SKN and its derivatives exert anti-inflammatory effects via diverse cellular mechanisms of action, including the suppression of mast cell degranulation, inhibition of the respiratory burst in neutrophils, and downregulation of lipopolysaccharide-induced

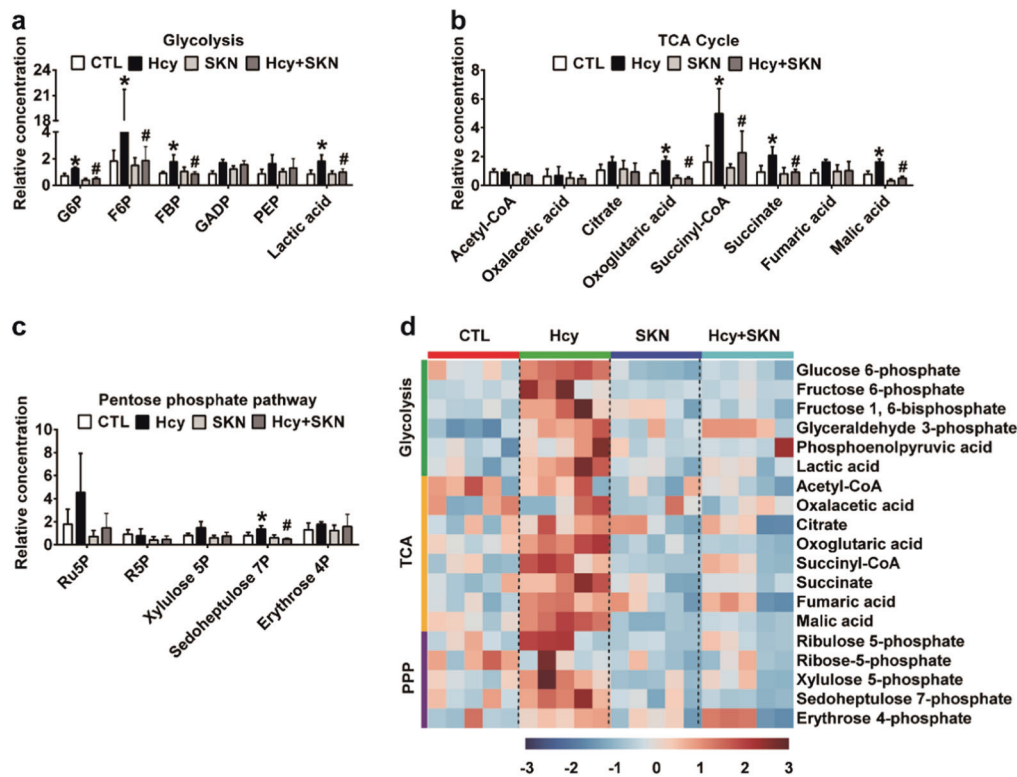


Fig. 4 SKN inhibits Hcy-induced CD4⁺ T cell glucose metabolism. Splenic CD4⁺ T cells were treated with or without SKN (0.2 μM) for 30 min and then stimulated with or without Hcy (100 μM) in the presence of anti-CD3 (1 μg/mL) for 24 h, following which T cell lysates were extracted and analyzed using LC-MS/MS to determine the levels of cellular metabolites. Relative levels of glycolytic intermediates (a) and intermediates in the TCA cycle (b) and the pentose phosphate pathway (c) are shown. G6P glucose-6-phosphate, F6P fructose-6-phosphate, FBP fructose-1,6-bisphosphate, GADP glyceraldehyde-3-phosphate, PEP phosphoenolpyruvate, Ru5P ribulose-5-phosphate, R5P ribose-5-phosphate, Xylulose 5P xylulose-5-phosphate, Sedoheptulose 7P sedoheptulose-7-phosphate, Erythrose 4P erythrose-4-phosphate (n = 5). d Heat map showing relative levels of metabolites involved in glycolysis, the TCA cycle, and the pentose phosphate pathway (n = 5). The data are shown as mean ± SD. One-way ANOVA followed by Tukey's test was used for multiple comparisons. *P < 0.05 compared with the CTL group; #P < 0.05 compared with the Hcy group

macrophage proinflammatory cytokine secretion [6]. Recently, we demonstrated that SKN also suppresses HHcy-induced B cell proliferation and immunoglobulin production [4]. Regarding T cell-associated diseases, SKN improved the macroscopic appearance and decreased cartilage destruction in established arthritis via reducing the expression of the T helper type 1 (Th1) cytokines TNF-α and interleukin (IL)-12 while simultaneously elevating the expression of the Th2 cytokines IL-10 and IL-4 [23]. In asthmatic mice, SKN inhibited allergic reaction and airway hyperresponsiveness, and an in vitro study revealed that the protective effects of SKN might result from the reduced expression of the Th2 cytokines IL-4 and IL-5 [24, 25]. Thus SKN efficiently mediates T cell-associated diseases by inducing different cytokine profiles. The present study provides new evidence that SKN inhibits HHcy-induced CD4⁺ T cell IFN-γ secretion and sheds light on the mechanisms by which SKN ameliorates atherosclerosis in HHcy-ApoE^{-/-} mice.

Th1 plays an atherogenic role by secreting IFN-γ, which has pathogenic effects, including the upregulation of adhesion molecules, induction of proinflammatory cytokines, and enhanced activation of macrophages and endothelial cells [26]. Based on preliminary data showing that SKN reduced IFN-γ gene expression in the aortas of HHcy-ApoE^{-/-} mice [4], we found that SKN reduced the HHcy-induced increase in CD4⁺ T cells in atherosclerotic plaques and decreased splenic CD4⁺ T cell IFN-γ secretion. Hcy-activated T cells promote macrophage migration by secreting IFN-γ [5]. The reduced number of macrophages in the atherosclerotic plaques of HHcy-ApoE^{-/-} mice might have

resulted from suppressed T cell IFN-γ secretion. In addition, IFN-γ mediates the polarization of macrophages to a proinflammatory state [18]. Therefore, SKN inhibits both splenic and vascular T cell inflammatory activation and might destroy T cell-macrophage inflammatory interactions, thus dampening the immune response and ameliorating atherosclerosis.

The crosstalk between pathways involved in the regulation of the immune and metabolic systems has become a research hotspot. Accumulating evidence has shown the critical role of metabolic pathways in regulating immune cell survival, proliferation, and effector functions [27]. As a potent inhibitor of PKM2, SKN efficiently inhibits the Warburg effect in both tumor cells and immune cells [7]. In addition, the potential of metabolomics in SKN-treated Huh7 human hepatoma cells has been investigated, the results of which improved knowledge on the mechanisms involved in the antitumor activity of SKN [10]. Whether cellular metabolism is changed in SKN-treated primary immune cells is unclear. In this study, we carried out comprehensive metabolomic profiling of Hcy-activated CD4⁺ T cells in the presence or absence of SKN to reveal the potential metabolic mechanism by which SKN modulates CD4⁺ T cell inflammatory activation. SKN effectively inhibited glucose metabolism and reduced the accumulation of lipids in Hcy-activated CD4⁺ T cells. Glucose metabolism produces enough substrates to meet the bioenergetic and biosynthetic demands of T cell activation. The pentose phosphate pathway and de novo lipid synthesis are both critical shunts of glucose metabolism [28]. In addition, ACC1 is a crucial enzyme for the de novo synthesis of lipids [29]. SKN reversed Hcy-induced ACC1

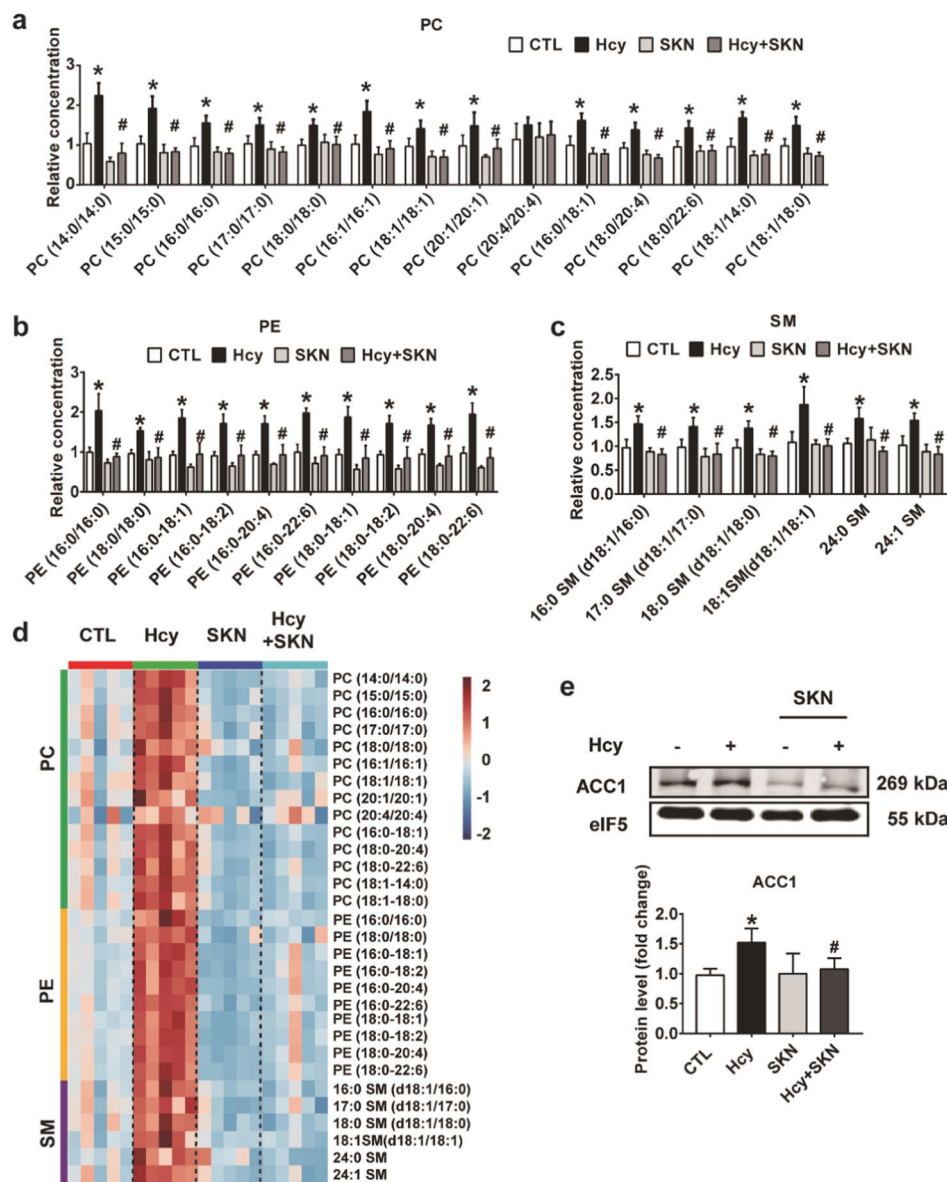


Fig. 5 SKN inhibits the Hcy-induced activation of the glycolytic-lipogenic axis in CD4⁺ T cells. Splenic CD4⁺ T cells were treated with or without SKN (0.2 μM) for 30 min and then stimulated with or without Hcy (100 μM) in the presence of anti-CD3 (1 μg/mL) for 24 h, following which T cell lysates were extracted and analyzed for cellular lipids using LC-MS/MS. Relative levels of the phospholipids PC (**a**), PE (**b**), and SM (**c**) are shown (*n* = 5). **d** Heat map showing an overview of lipidomic alterations (*n* = 5). **e** The protein level of ACC1 was detected by western blotting (*n* = 7). The data are shown as mean ± SD. One-way ANOVA followed by Tukey's test was used for multiple comparisons. **P* < 0.05 compared with the CTL group; #*P* < 0.05 compared with the Hcy group

upregulation. The critical role of the glycolytic-lipogenic axis in modulating T cell inflammatory activation was emphasized in our previous study [12]. PC and PE are the major components of biomembranes; SM is a major component of lipid rafts and important for cell signaling transduction [19, 30]. The SKN-induced inhibition of de novo lipid synthesis might lead to reduced biomembrane synthesis and suppressed cell signaling transduction. Taken together, these results suggest that SKN inhibits glucose metabolism and suppresses related pathophysiological processes. This study is the first to elucidate the mechanism by which SKN regulates intracellular metabolism in T lymphocytes.

Metabolism in tumor cells results in a specific tumor microenvironment with limited nutrients and accumulated waste products, which in turn impacts T cell metabolism and functions, ultimately leading to tumorigenesis. Modulating the metabolism of T cells or tumor cells has been shown to be a promising method

of tumor therapy [31]. However, there have been few studies on potential strategies to target T cell metabolism in cardiovascular diseases, especially natural and herbal pharmacological intervention. Increased glucose flux has been reported in the atherosclerotic plaques of ApoE^{-/-} mice, indicating an association between immune cell metabolism and atherogenesis. A previous study showed that glucose transporter 1-deficient bone marrow transplantation prevented myelopoiesis and atherosclerosis in ApoE^{-/-} mice [32]. A recent study demonstrated that PKM2 boosts IL-6 and IL-1β production in monocytes and macrophages from patients with atherosclerotic coronary artery disease [33]. Our recent study demonstrated that HHcy promotes atherosclerosis in ApoE^{-/-} mice via PKM2-dependent CD4⁺ T cell inflammatory activation [12]. These findings indicate that immune cell metabolism may be a potential target in cardiovascular diseases. However, all these studies are based on gene knockout

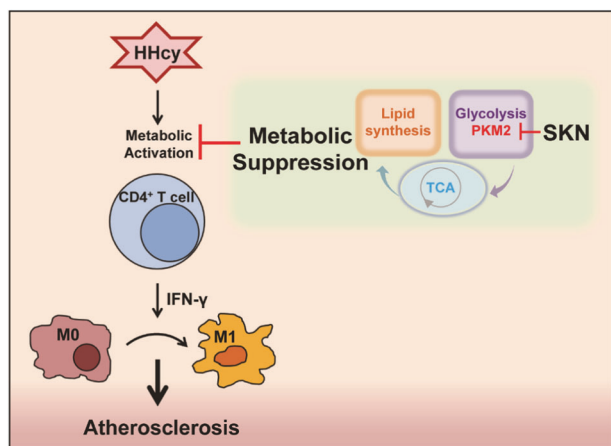


Fig. 6 A working model by which SKN ameliorates atherosclerosis by inhibiting CD4⁺ T cell metabolic activation. Hcy enhances glucose metabolism and the glycolytic–lipogenic axis in CD4⁺ T cells to promote IFN- γ secretion, which promotes macrophage proinflammatory polarization and finally accelerates atherosclerosis. Inhibition of PKM2 by SKN prevents these effects

mice. In the present study, we provide direct evidence that the phytochemical component SKN may be an effective cardiovascular therapeutic agent targeting CD4⁺ T cell metabolism. In addition, SKN can also modulate macrophages, B cells, and VSMCs, which together may contribute to ameliorating atherosclerosis in HHcy-ApoE^{-/-} mice in vivo [4, 8, 22]. The systemic effects of SKN in vivo require further study in the future.

Collectively, our results suggest SKN as a promising therapeutic agent for the treatment of HHcy-accelerated atherosclerosis, which is at least partly associated with reduced CD4⁺ T cell inflammation mediated by suppression of the glycolytic–lipogenic axis. Because of the fundamental importance of immune cell metabolism in physiology and pathophysiology, the results of this study may have broad implications.

ACKNOWLEDGEMENTS

This work was supported by the National Natural Science Foundation of China (Nos. 91739303, 81770445).

AUTHOR CONTRIBUTIONS

SLL, JF, and XW designed and supervised the research; SLL performed the research, analyzed data, prepared figures, and wrote the manuscript; GHD, JCD, HYL, and BL participated in the experiments; JY, XLM, and YTM assisted in the research; and QBX, JCD, and CTJ provided advice.

ADDITIONAL INFORMATION

The online version of this article (<https://doi.org/10.1038/s41401-019-0308-7>) contains supplementary material, which is available to authorized users.

Competing interests: The authors declare no competing interests.

REFERENCES

- Lozano R, Naghavi M, Foreman K, Lim S, Shibuya K, Aboyans V, et al. Global and regional mortality from 235 causes of death for 20 age groups in 1990 and 2010: a systematic analysis for the Global Burden of Disease Study 2010. *Lancet*. 2012;380:2095–128.
- McCully KS. Homocysteine and vascular disease. *Nat Med*. 1996;2:386–9.
- Guthikonda S, Haynes WG. Homocysteine as a novel risk factor for atherosclerosis. *Curr Opin Cardiol*. 1999;14:283–91.
- Deng J, Lu S, Liu H, Liu B, Jiang C, Xu Q, et al. Homocysteine activates B cells via regulating PKM2-dependent metabolic reprogramming. *J Immunol*. 2017;198:170–83.

- Ma K, Lv S, Liu B, Liu Z, Luo Y, Kong W, et al. CTLA4-IgG ameliorates homocysteine-accelerated atherosclerosis by inhibiting T-cell overactivation in apoE^{-/-} mice. *Cardiovasc Res*. 2013;97:349–59.
- Andujar I, Rios JL, Giner RM, Recio MC. Pharmacological properties of shikonin - a review of literature since 2002. *Planta Med*. 2013;79:1685–97.
- Chen J, Xie J, Jiang Z, Wang B, Wang Y, Hu X. Shikonin and its analogs inhibit cancer cell glycolysis by targeting tumor pyruvate kinase-M2. *Oncogene*. 2011;30:4297–306.
- Yang L, Xie M, Yang M, Yu Y, Zhu S, Hou W, et al. PKM2 regulates the Warburg effect and promotes HMGB1 release in sepsis. *Nat Commun*. 2014;5:4436.
- Xie M, Yu Y, Kang R, Zhu S, Yang L, Zeng L, et al. PKM2-dependent glycolysis promotes NLRP3 and AIM2 inflammasome activation. *Nat Commun*. 2016;7:13280.
- Spyrelli ED, Kyriazou AV, Virgiliou C, Nakas A, Deda O, Papageorgiou VP, et al. Metabolic profiling study of shikonin's cytotoxic activity in the Huh7 human hepatoma cell line. *Mol Biosyst*. 2017;13:841–51.
- Zhang X, Hu W, Wu F, Yuan X, Hu J. Shikonin inhibits TNF-alpha-induced growth and invasion of rat aortic vascular smooth muscle cells. *Can J Physiol Pharmacol*. 2015;93:615–24.
- Lu S, Deng J, Liu H, Liu B, Yang J, Miao Y, et al. PKM2-dependent metabolic reprogramming in CD4(+) T cells is crucial for hyperhomocysteinemia-accelerated atherosclerosis. *J Mol Med (Berl)*. 2018;96:585–600.
- Dai XY, Cai Y, Sun W, Ding Y, Wang W, Kong W, et al. Intermedin inhibits macrophage foam-cell formation via tristetrarprolin-mediated decay of CD36 mRNA. *Cardiovasc Res*. 2014;101:297–305.
- Christofk HR, Vander Heiden MG, Wu N, Asara JM, Cantley LC. Pyruvate kinase M2 is a phosphotyrosine-binding protein. *Nature*. 2008;452:181–6.
- Feng J, Zhang Z, Kong W, Liu B, Xu Q, Wang X. Regulatory T cells ameliorate hyperhomocysteinemia-accelerated atherosclerosis in apoE^{-/-} mice. *Cardiovasc Res*. 2009;84:155–63.
- Liu Z, Luo H, Zhang L, Huang Y, Liu B, Ma K, et al. Hyperhomocysteinemia exaggerates adventitial inflammation and angiotensin II-induced abdominal aortic aneurysm in mice. *Circ Res*. 2012;111:1261–73.
- Rudd CE, Taylor A, Schneider H. CD28 and CTLA-4 coreceptor expression and signal transduction. *Immunol Rev*. 2009;229:12–26.
- Ivashkiv LB. IFN γ : signalling, epigenetics and roles in immunity, metabolism, disease and cancer immunotherapy. *Nat Rev Immunol*. 2018;18:545–58.
- Lochner M, Berod L, Sparwasser T. Fatty acid metabolism in the regulation of T cell function. *Trends Immunol*. 2015;36:81–91.
- Yang J, Wang Z, Chen DL. Shikonin ameliorates isoproterenol (ISO)-induced myocardial damage through suppressing fibrosis, inflammation, apoptosis and ER stress. *Biomed Pharmacother*. 2017;93:1343–57.
- Han T, Zhang G, Yan D, Yang H, Ma T, Ye Z. Modulation of plasminogen activator inhibitor-1 (PAI-1) by the naphthoquinone shikonin. *Fitoterapia*. 2016;113:117–22.
- Yoshida LS, Kawada T, Irie K, Yuda Y, Himi T, Ikemoto F, et al. Shikonin directly inhibits nitric oxide synthases: possible targets that affect thoracic aorta relaxation response and nitric oxide release from RAW 264.7 macrophages. *J Pharmacol Sci*. 2010;112:343–51.
- Dai Q, Fang J, Zhang FS. Dual role of shikonin in early and late stages of collagen type II arthritis. *Mol Biol Rep*. 2009;36:1597–604.
- Lee CC, Wang CN, Lai YT, Kang JJ, Liao JW, Chiang BL, et al. Shikonin inhibits maturation of bone marrow-derived dendritic cells and suppresses allergic airway inflammation in a murine model of asthma. *Br J Pharmacol*. 2010;161:1496–511.
- Lee CC, Kang JJ, Chiang BL, Wang CN, Cheng YW. Shikonin inhibited mitogen-activated IL-4 and IL-5 production on EL-4 cells through downregulation of GATA-3 and c-Maf induction. *Life Sci*. 2011;89:364–70.
- Hansson GK, Robertson AK, Soderberg-Naucler C. Inflammation and atherosclerosis. *Annu Rev Pathol*. 2006;1:297–329.
- O'Sullivan D, Pearce EL. Targeting T cell metabolism for therapy. *Trends Immunol*. 2015;36:71–80.
- Pearce EL, Poffenberger MC, Chang CH, Jones RG. Fueling immunity: insights into metabolism and lymphocyte function. *Science*. 2013;342:1242–454.
- Berod L, Friedrich C, Nandan A, Freitag J, Hagemann S, Harmrolfs K, et al. De novo fatty acid synthesis controls the fate between regulatory T and T helper 17 cells. *Nat Med*. 2014;20:1327–33.
- Simons K, Ikonen E. Functional rafts in cell membranes. *Nature*. 1997;387:569–72.
- Beckermann KE, Dudzinski SO, Rathmell JC. Dysfunctional T cell metabolism in the tumor microenvironment. *Cytokine Growth Factor Rev*. 2017;35:7–14.
- Sarrazay V, Viaud M, Westerterp M, Ivanov S, Giorgetti-Peraldi S, Guinamard R, et al. Disruption of Glut1 in hematopoietic stem cells prevents myelopoiesis and enhanced glucose flux in atheromatous plaques of ApoE^{-/-} mice. *Circ Res*. 2016;118:1062–77.
- Shirai T, Nazarewicz RR, Wallis BB, Yanes RE, Watanabe R, Hilhorst M, et al. The glycolytic enzyme PKM2 bridges metabolic and inflammatory dysfunction in coronary artery disease. *J Exp Med*. 2016;213:337–54.